

Ciguatoxins activate specific cold pain pathways to elicit burning pain from cooling

Irina Vetter¹, Filip Touska^{2,3},
Andreas Hess⁴, Rachel Hinsbey⁵,
Simon Sattler², Angelika Lampert²,
Marina Sergejeva⁴, Anastasia Sharov⁶,
Lindon S Collins⁶, Mirjam Eberhardt²,
Matthias Engel², Peter J Cabot⁶,
John N Wood⁵, Viktorie Vlachová³,
Peter W Reeh², Richard J Lewis¹ and
Katharina Zimmermann^{2,*}

¹Institute for Molecular Bioscience, The University of Queensland, St Lucia, Queensland, Australia, ²Department of Physiology and Pathophysiology, Friedrich-Alexander-University Erlangen-Nuremberg, Erlangen, Germany, ³Department of Cellular Neurophysiology, Institute of Physiology, Academy of Sciences of the Czech Republic, Prague 4, Czech Republic, ⁴Department of Experimental and Clinical Pharmacology and Toxicology, Friedrich-Alexander-University Erlangen-Nuremberg, Erlangen, Germany, ⁵Wolfson Institute for Biomedical Research, University College London, London, UK and ⁶School of Pharmacy, The University of Queensland, Woolloongabba, Queensland, Australia

Ciguatoxins are sodium channel activator toxins that cause ciguatera, the most common form of ichthyosarcotoxism, which presents with peripheral sensory disturbances, including the pathognomonic symptom of cold allodynia which is characterized by intense stabbing and burning pain in response to mild cooling. We show that intraplantar injection of P-CTX-1 elicits cold allodynia in mice by targeting specific unmyelinated and myelinated primary sensory neurons. These include both tetrodotoxin-resistant, TRPA1-expressing peptidergic C-fibres and tetrodotoxin-sensitive A-fibres. P-CTX-1 does not directly open heterologously expressed TRPA1, but when co-expressed with Na_v channels, sodium channel activation by P-CTX-1 is sufficient to drive TRPA1-dependent calcium influx that is responsible for the development of cold allodynia, as evidenced by a large reduction of excitatory effect of P-CTX-1 on TRPA1-deficient nociceptive C-fibres and of ciguatoxin-induced cold allodynia in TRPA1-null mutant mice. Functional MRI studies revealed that ciguatoxin-induced cold allodynia enhanced the BOLD (Blood Oxygenation Level Dependent) signal, an effect that was blunted in TRPA1-deficient mice, confirming an important role for TRPA1 in the pathogenesis of cold allodynia.

The EMBO Journal (2012) 31, 3795–3808. doi:10.1038/emboj.2012.207; Published online 31 July 2012

Subject Categories: neuroscience; molecular biology of disease

Keywords: ciguatoxin; cold allodynia; Na_v; nociceptor; TRPA1

*Corresponding author. Department of Physiology and Pathophysiology, Friedrich-Alexander-University Erlangen-Nuremberg, Universitaetsstrasse 17, 91054 Erlangen, Germany. Tel.: +49 9131 8522491; Fax: +49 9131 8522497; E-mail: zimmermann@physiologie1.uni-erlangen.de

Received: 17 November 2011; accepted: 28 June 2012; published online: 31 July 2012

Introduction

In 1774, when Captain James Cook was exploring the coast of the New Hebrides, sailors aboard the *HMS Resolution* experienced a peculiar kind of poisoning after eating fish (Beaglehole, 1961). The initial symptoms occurred soon after their meal and consisted of gastrointestinal effects, in particular intense nausea, diarrhoea and abdominal pain. However, subjectively among the most distressing symptoms were neurological disturbances affecting the central nervous system, and also peripheral sensory disturbances including paraesthesias, localized intense pruritus and several painful dysaesthesias. The most prominent of these was a long-lasting sensory disorder reminiscent of cold allodynia, where exposure to cool objects or water induced severe burning pain and electric shock-like sensations (Bagnis *et al*, 1979). This form of fish poisoning, known as ‘ciguatera’ occurs worldwide in circumtropical regions, with the global incidence estimated to be as high as 50 000–500 000 cases annually (Fleming *et al*, 1998), making it the most common form of non-bacterial food poisoning. Ciguatera is caused by ciguatoxins, a group of lipophilic, polycyclic polyether toxins that are produced by dinoflagellates of the genus *Gambierdiscus* and bioaccumulate through the marine food chain (Lewis and Holmes, 1993). Structurally related variants of ciguatoxin exist in the Caribbean, the Indian and Pacific Ocean (C-CTX, I-CTX and P-CTX, respectively). Of these, P-CTX-1 is the most potent and thought to be responsible for the majority of neurological symptoms associated with ciguatera in the Pacific (Lewis, 2001). Ciguatoxins have previously been recognized as potent activators of voltage-gated sodium channels (Na_v), however, little is known about the mechanisms by which they produce cold allodynia. In this study, we sought to identify the sensory neuronal populations mediating these symptoms and to elucidate the cellular and molecular basis of ciguatoxin-induced cold allodynia.

Results

A mouse model reproduces ciguatoxin-induced cold allodynia

To elucidate the molecular pathways through which P-CTX-1 selectively targets neurons to elicit pain and cold allodynia, we established a new animal model of ciguatoxin-induced peripheral sensory disturbances. Systemic administration of ciguatoxin by the intraperitoneal (i.p.) or oral route in mice is associated with diarrhoea, hypothermia, salivation, lacrimation, muscle weakness, decreased motor activity and cyanosis (Hoffman *et al*, 1983). Importantly, systemic administration of ciguatoxin also results in a decrease in nerve conduction velocity and blunts the corneal and nociceptive withdrawal reflex. Therefore, in order to avoid systemic effects of ciguatoxin and to isolate the actions of

CTX on peripheral sensory neurons, we used administration of low nanomolar solutions of P-CTX-1 (1–10 nM) by shallow intraplantar (i.pl.) injection. P-CTX-1 caused rapid, dose-dependent development of spontaneous pain in C57BL/6 mice, evidenced by flinching, lifting, shaking and licking of the affected hind paw that was accompanied by the development of cold allodynia (Figure 1A–D). Specifically, 45–60 min after i.pl. administration of P-CTX-1 the spontaneous nocifensive behaviour ceased, revealing prominent signs of cold allodynia that comprised paw lifting, licking, flinching and shaking observed at 20°C or cooler (Figure 1C). In contrast, at elevated temperatures up to 42°C, these animals displayed little or no nocifensive behaviour (Figure 1C). In addition, no mechanical allodynia was observed after i.pl. injection of P-CTX-1, consistent with the absence of mechanical sensitization in nociceptive C-fibres recorded from isolated rat saphenous nerve preparations (Supplementary Figure 1).

This new animal model thus produces behavioural responses that parallel the human symptomatology of ciguatera, and confirms the exquisite sensitivity of peripheral sensory neurons to P-CTX-1. Striking effects were observed upon i.pl. administration of as little as 5–500 pg of P-CTX-1, making this marine polyether toxin one of the most potent pro-algesic compounds known, with much higher doses of capsaicin (2500 ng/paw), bradykinin (300 ng/paw) or NGF (50 ng/paw) required to achieve comparable effects (Amaya *et al*, 2006).

TRPA1-expressing DRG neurons show exquisite sensitivity to P-CTX-1

Cold allodynia is a symptom reported by a high proportion (76–94%) of ciguatera sufferers, suggesting that ciguatoxin activates specific nociceptive pathways that are intrinsically linked to the development of cold allodynia. To characterize the sensory neuronal populations targeted by P-CTX-1, we used a high-content bioimaging assay that allows live-cell Ca^{2+} imaging to be combined with immunohistochemistry at the level of single cells (Figure 2A and B; Supplementary Figure 2). In cultured mouse dorsal root ganglion (DRG) neurons, 51% of neurons responded to stimulation with P-CTX-1 (1 nM) with an increase in intracellular Ca^{2+} (Figure 2A; Supplementary Figure 2). Immunohistochemical characterization of the ciguatoxin-sensitive population using previously characterized antibodies (Supplementary Table 1) showed that 42% of NF200-positive (a marker of large myelinated A-fibre-associated cells) and 66% of peripherin-positive (a marker of unmyelinated C-fibre and thinly myelinated A δ -fibre-associated cells) neurons responded to the addition of P-CTX-1, while IB4-positive DRG neurons largely defined the ciguatoxin-insensitive neuronal population (12% were ciguatoxin sensitive). Interestingly, virtually all CGRP- (82%) and TRPA1- (95%) positive cells were activated by low P-CTX-1 concentrations (1 nM), suggesting that TRPA1-expressing peptidergic neurons play a pivotal role in the symptomatology of ciguatera. Higher concentrations of P-CTX-1 were less discriminating and increasingly

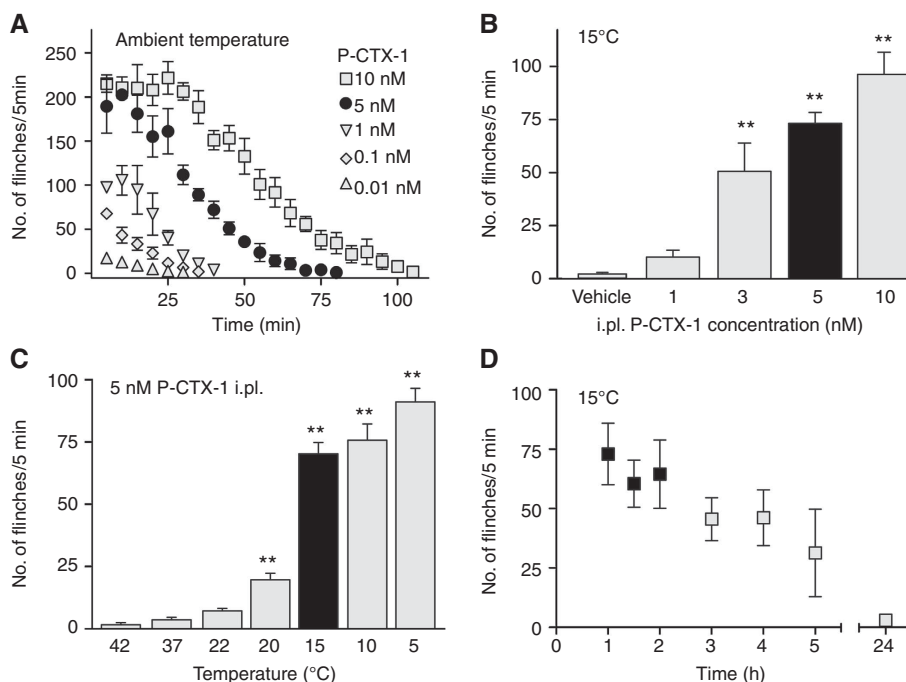


Figure 1 A mouse model reproduces ciguatoxin-induced cold allodynia. (A) Intraplantar administration of P-CTX-1 caused dose-dependent spontaneous pain behaviour at room temperature, evidenced by increased number of paw lifts, licks, flinches and shakes. This spontaneous nocifensive behaviour subsided within ~60–100 min ($n = 6$ each). (B) P-CTX-1-induced cold allodynia—assessed after spontaneous pain had faded—appeared dose-dependent (40 μ l volume per i.pl. injection, measured at 15°C; $n = 5$ –12 animals/group) and (C) temperature-dependent (5 nM; 40 μ l by i.pl. injection; $n = 6$ –23 animals/group). (D) Time course of 5 nM P-CTX-1-induced cold allodynia at 15°C: cold allodynia persisted for several hours but subsided within 24 h ($n = 6$). Black bars in (B, C): for all further experiments, 5 nM was chosen and cold allodynia was assessed at 15°C; black squares in (D) indicate the timeframe in which cold allodynia was assessed in (B–D) (and experiments underlying Figures 4L and 5A, 5F). Statistical significance was determined using a one-way ANOVA with Dunnett’s *post hoc* comparison; ** $P < 0.01$ compared to 37°C or vehicle. Data are presented as mean \pm s.e.m.

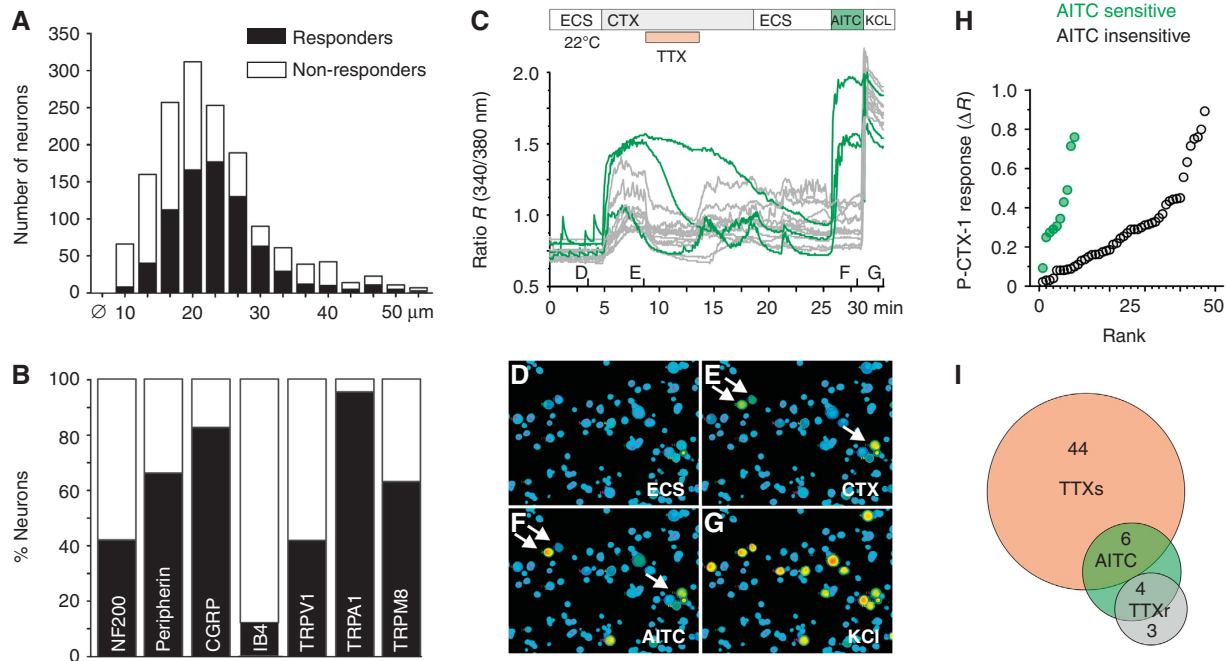


Figure 2 Characterization of ciguatoxin-sensitive sensory neuron populations. (A) DRG neurons responding to P-CTX-1 (1 nM) were predominantly medium to large sized. (B) Immunohistochemical characterization of ciguatoxin-sensitive DRG neurons using antibodies for NF200, peripherin, CGRP, IB4, TRPV1, TRPA1 and TRPM8. Black bars, P-CTX-1 responders; white bars, P-CTX-1 non-responders. (C) Ca^{2+} responses at 22°C in rat DRG neurons and representative images after stimulation with (D) extracellular solution (ECS), (E) 1 nM P-CTX-1, 300 nM tetrodotoxin (TTX), (F) 25 μM allyl isothiocyanate (AITC) and (G) 60 mM potassium chloride. Arrows in (E, F) indicate P-CTX-1-sensitive neurons marked green in (C). (H) AITC-sensitive neurons (green) showed significantly larger ciguatoxin-induced Ca^{2+} responses than AITC-insensitive neurons (grey; $P=0.005$, Wilcoxon-matched pairs test). (I) Venn diagram illustrating pharmacological characteristics of all cells with calcium increase upon P-CTX-1 application. The P-CTX-1-induced calcium increase could be blocked to at least 50% by TTX (300 nM) in the majority of cells.

excited remaining neuronal populations, with 76% of DRG neurons excited by 5 nM P-CTX-1 (Supplementary Figure 3).

Preferential activation of TRPA1-expressing cells by P-CTX-1 was further confirmed by pharmacological characterization of cultured DRG neurons using ratiometric calcium imaging. Here, cells with functional TRPA1 expression, tested by application of the agonist allyl isothiocyanate (AITC, 25 μM), showed the largest calcium increase in response to P-CTX-1 (Figure 2C–H). Furthermore, the CTX-induced calcium increase was reduced by tetrodotoxin (TTX; 300 nM to at least 50%) in the majority of cells (81%; Figure 2C and I), consistent with the predominant pharmacological action of P-CTX-1 on TTX-sensitive (TTXs) voltage-gated sodium channels (VGSC). Based on these observations, we next assessed the contribution of TRPA1 to neuronal cold responses and cold sensitization induced by ciguatoxin in wild-type (*wt*) and TRPA1-deficient mice (Figure 3). In cultured mouse DRG neurons from *wt* and TRPA1 $-/-$ animals, lowering the temperature from 35° to 15°C elicited cold-induced Ca^{2+} responses in 16.5% of *wt* and 6.9% of TRPA1 $-/-$ neurons. These cold responses are most likely mediated by TRPM8 and other putative cold sensors, such as TRPC5 (Bautista *et al*, 2007; Zimmermann *et al*, 2011). Interestingly, the Ca^{2+} responses of these cold-sensitive neurons were not significantly affected by P-CTX-1 (Figure 3). However, P-CTX-1 elicited a striking cold sensitization in 39% of previously cold-insensitive neurons (Figure 3D). This effect was less pronounced in the absence of P-CTX-1 (Figure 3E; 8.9% sensitized to cold) and was dependent on TRPA1, as

ciguatoxin-mediated *de-novo* sensitization to cooling was absent in DRG neurons from TRPA1 $-/-$ mice (Figure 3D; 6.6% sensitized to cold).

To further characterize the contribution of TRPA1 to ciguatoxin-induced peripheral sensitization, we performed *ex-vivo* recordings from murine skin-saphenous nerve preparations. This preparation permits single-fibre recordings of propagated action potentials arising from sensory stimulation directly to the receptive fields of C- and A-fibres (Zimmermann *et al*, 2009). Application of as little as 0.1 nM P-CTX-1 at a bath temperature of 28–30°C induced ongoing activity in the majority of C-fibre nerve endings and at 0.5 nM, strong and long-lasting action potential bursts appeared in some fibres (Figure 4A). This is consistent with a shift of the dynamic range of ciguatoxin-modified C-fibres, and reminiscent of the thermal sensitization observed previously in C-fibres treated with menthol (Zimmermann *et al*, 2011). The ongoing activity induced by P-CTX-1 at skin temperature ceased upon further cooling (Figure 4A), likely due to inactivation of TTXs VGSC that eventually leads to quiescent C-fibres (Zimmermann *et al*, 2007). Importantly, these ciguatoxin-mediated effects on C-fibres were greatly reduced in skin-nerve preparations from TRPA1 $-/-$ mice (Figure 4A–C; see Supplementary Table 2).

A direct effect of P-CTX-1 on TRPA1 was ruled out as P-CTX-1 at concentrations up to 100 nM failed to directly activate or sensitize Ca^{2+} responses mediated through heterologous expressed hTRPA1 (Figure 4D and E), and did not affect TRPA1 currents in whole-cell patch-clamp recordings

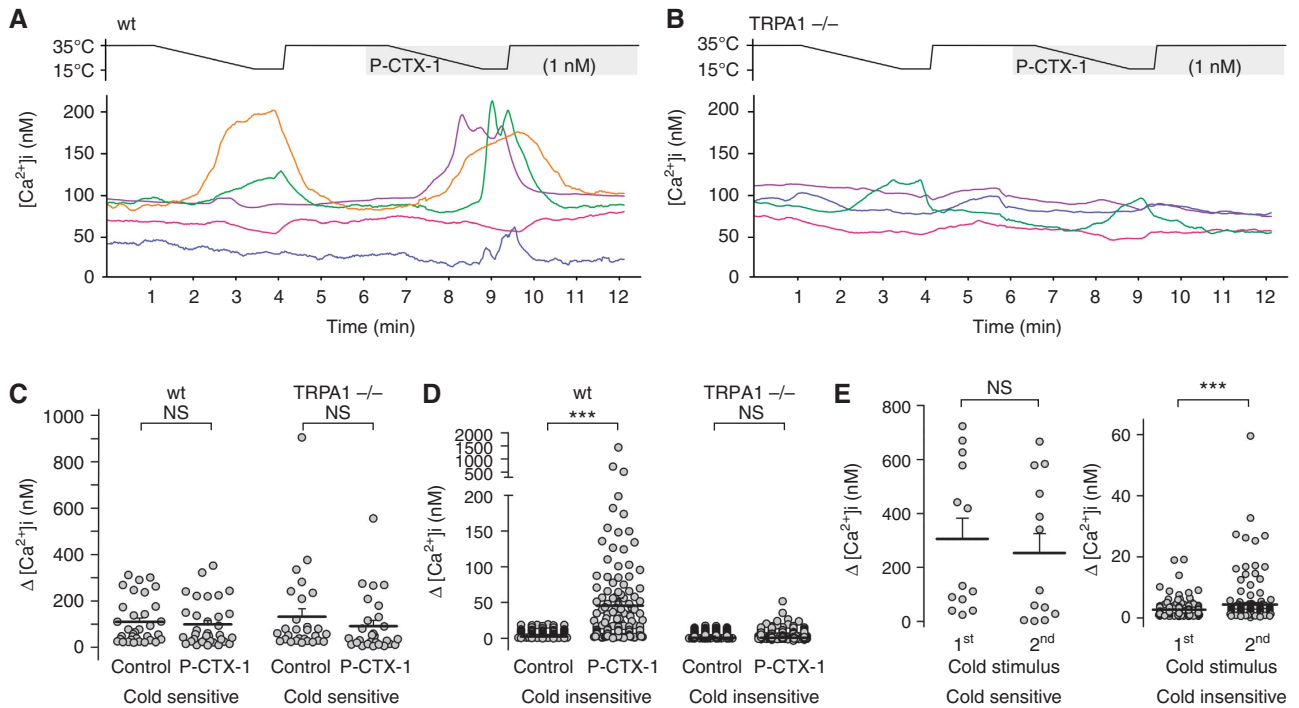


Figure 3 Ciguatoxin induces new sensitivity to cold in cultured DRG neurons via TRPA1. (A–D) Cold responses and cold sensitization by P-CTX-1 (1 nM) in cultured DRG neurons from (A) *wt* and (B) TRPA1^{-/-} mice. (C) Ca²⁺ responses of cold-sensitive cultured neurons were not significantly affected by P-CTX-1 but (D) P-CTX-1 induced novel sensitivity to cooling in previously cold-insensitive neurons, which was absent in TRPA1^{-/-} neurons. (E) Cold sensitization to a second cold stimulus was less pronounced in *wt* neurons in the absence of P-CTX-1. Statistical significance was determined using a paired, two-tailed Student's *t*-test; **P* < 0.05; ****P* < 0.001; NS, *P* > 0.05. Data are presented as mean ± s.d.

(Supplementary Figure 4). Based on these results, it appears that ciguatoxin-induced membrane depolarization and membrane oscillations, which was determined to be +10 mV on average in cultured DRG neurons recorded in current-clamp configuration (Figure 4F–H), in combination with a cooling-induced leftward shift of the voltage dependence of TRPA1 activation reported previously (Karashima *et al*, 2009), are sufficient to activate TRPA1 in cold nociceptors which is then perceived as the burning pain of cold allodynia. In support of this hypothesis, in HEK293 cells co-expressing TRPA1 and the TTXs Na_v1.7 or Na_v1.3, stimulation by P-CTX-1 or the Na_v activator veratridine at 20°C generated TRPA1-mediated Ca²⁺ responses that were blocked by the TRPA1 antagonist HC030031, the sodium channel blocker tetracaine, and were absent in cells only expressing TTXs Na_v or TRPA1 (Figure 4I–K; Supplementary Figure 5). The contribution of TRPA1 to ciguatoxin-induced peripheral sensitization was also critical *in vivo*, with the development of ciguatoxin-mediated cold allodynia significantly decreased in TRPA1^{-/-} mice. In contrast, cold allodynia was unaltered in mice lacking TRPM8 or TRPV1 (Figure 4L), or the recently identified cold transducer TRPC5 (data not shown). In addition, the TRPM8-specific antagonist AMTB did not affect ciguatoxin-induced cold allodynia, and no reduction in spontaneous pain was apparent in TRPM8 knockout animals (Figure 4L).

Both Na_v 1.8 and TTXs Na_v subtypes are effectors of ciguatoxin-induced cold allodynia

Based on previous reports that the TTX-resistant (TTXr) Na_v1.8 is essential for the detection and perception of

noxious cold pain (Zimmermann *et al*, 2007; Abrahamsen *et al*, 2008), we assessed the contribution of Na_v1.8 to ciguatoxin-induced cold allodynia. In contrast to previous studies reporting negligible responses of Na_v1.8^{-/-} animals in response to noxious cold stimuli (Zimmermann *et al*, 2007), we found only a partial inhibition of ciguatoxin-induced cold allodynia in Na_v1.8^{-/-} animals (35.5% reduction of cold allodynia), which was mimicked by i.p.l. administration of the Na_v1.8 blocker A803467 (10 μM, 36.4% reduction of cold allodynia) and no significant effect in Na_v1.9^{-/-} mice (Figure 5A). Similar results were obtained in mice with diphtheria toxin-mediated ablation of Na_v1.8-expressing nociceptors (Na_v1.8-DTA), where residual ciguatoxin-induced cold allodynia persisted (48.8% remaining cold allodynia; Figure 5A) despite an almost complete loss of noxious cold responses in these animals (Abrahamsen *et al*, 2008). Consistent with ablation of predominantly Na_v1.8-expressing C-fibres in the Na_v1.8-DTA mice, *ex-vivo* recordings from C-fibres devoid of Na_v1.8 showed an 85–90% reduction of ciguatoxin-induced activity (Figure 5B; see Supplementary Table 2), with the residual ciguatoxin-induced action potentials now entirely TTXs. This result was congruent with an analogous ~15% attenuation of the CTX effect by TTX in *wt* C-fibres. These results reveal that both TTXr Na_v1.8 and TTXs Na_v contribute to ciguatoxin-induced cold allodynia, and that in addition to Na_v1.8-expressing C-fibres, TTXs pathways contribute to ciguatoxin-induced cold allodynia.

Indeed, in A-fibres, treatment with P-CTX-1 caused strong ongoing activity and cold sensitization that was completely blocked by TTX (Figure 5C and D), consistent with previous

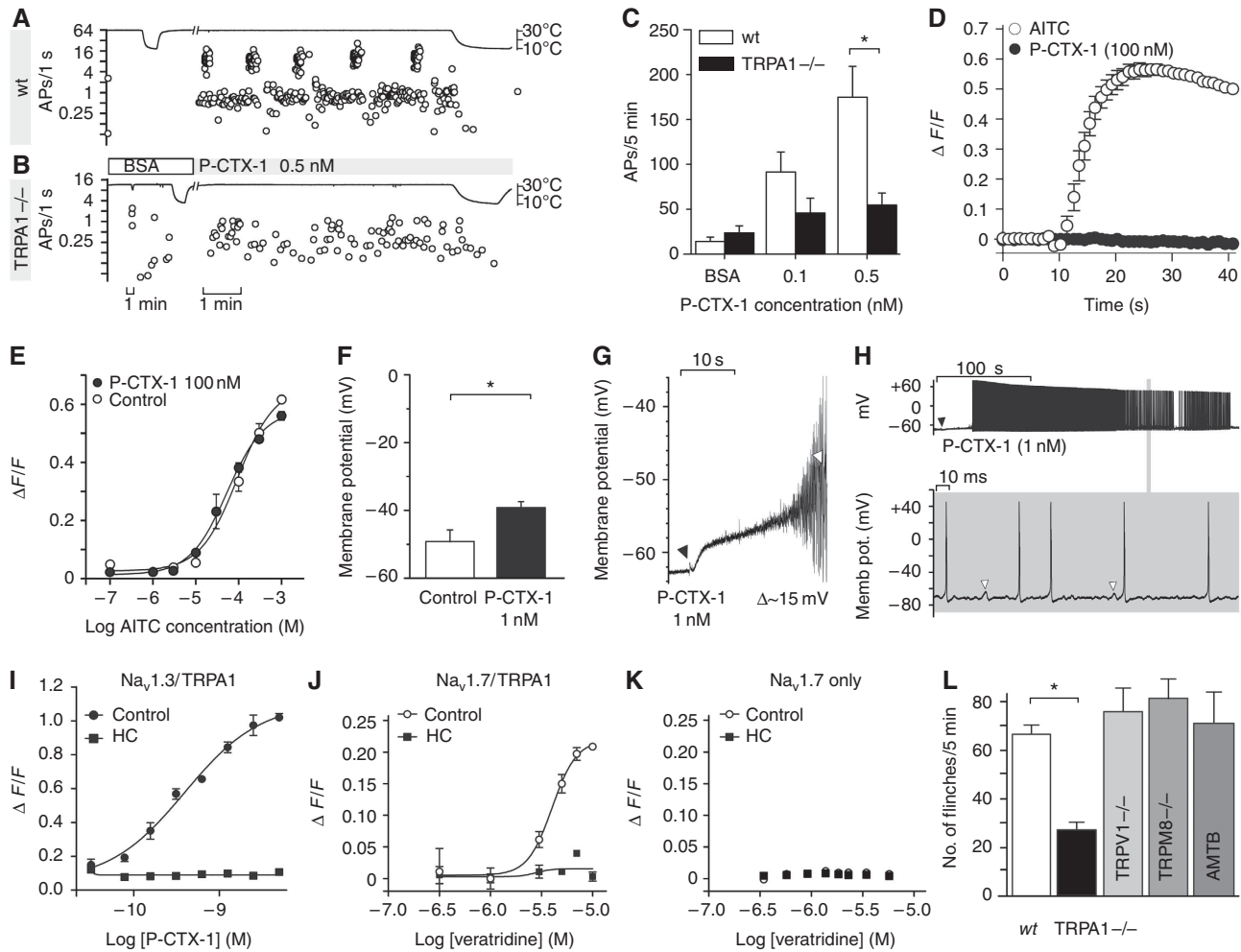


Figure 4 TRPA1 mediates ciguatoxin-induced cold allodynia. (A–C) P-CTX-1-induced ongoing activity in single C-fibres recorded from murine skin-saphenous nerve preparations is markedly reduced in preparations from TRPA1-deficient mice. Representative recording from (A) a wt and (B) a TRPA1^{-/-} nociceptor. (C) Cumulative ciguatoxin-induced action potentials in 5 min from wt (white bars, *n* = 11) and TRPA1^{-/-} (black bars, *n* = 12) animals. In all, 8/10 (80%) of wt fibres and 5/12 (42%) of TRPA1^{-/-} fibres more than doubled the number of cumulative actions potentials in response to 0.5 nM P-CTX-1. (D, E) P-CTX-1 neither activates nor potentiates heterologously expressed TRPA1. Cos-1 cells heterologously expressing TRPA1 were loaded with Fluo-4 and Ca²⁺ responses to P-CTX-1 and AITC measured using a FLIPR^{TETRA} plate reader. (D) In TRPA1-expressing cells, P-CTX-1 (100 nM) did not elicit increases in intracellular Ca²⁺, while AITC (300 μM) caused rapid Ca²⁺ increases. (E) Pretreatment for 5 min with 100 nM P-CTX-1 did not significantly affect the AITC concentration-response curve. Data represent *n* = 3 wells and are representative of three independent experiments. (F) P-CTX-1 applied at 1 nM depolarized the membrane potential of cultured DRG neurons recorded in current-clamp mode by 10 mV on average (*n* = 6). (G, H) Representative examples of P-CTX-1 induced depolarization. (G) Application of P-CTX-1 (black arrow) caused depolarization of membrane potential followed by action potential firing (white arrow: first action potential). (H) Upper panel: ciguatoxin-induced depolarization rapidly leads to series of action potentials. Detail expanded in lower panel: white arrows: membrane oscillations, frequently followed by action potentials. (I–K) P-CTX-1 and veratridine elicit TRPA1-mediated calcium responses in HEK cells co-expressing Na_v1.3 or Na_v1.7 and TRPA1. HEK293 cells were loaded with Fluo-4 and Ca²⁺ responses at 20°C measured using a FLIPR^{TETRA} plate reader. (I) Stimulation with P-CTX1 caused an increase in Ca²⁺ that was blocked by the TRPA1 inhibitor HC030031 (100 μM) and absent in cells only expressing Na_v1.3 or TRPA1. Expression of functional TRPA1 and Na_v was verified using AITC or membrane potential dye, respectively; *n* = 6 wells in *n* = 5 independent experiments. (J) Stimulation with veratridine caused a concentration-dependent increase in Ca²⁺ (open circles) that was blocked by the TRPA1 inhibitor HC030031 (100 μM; black squares). (K) Veratridine did not elicit Ca²⁺ responses in HEK293 cells expressing only TRPA1 (not shown) or only Na_v1.7. Data are presented as mean ± s.e.m. with *n* = 15 wells and are representative of two independent experiments. (L) Compared to wt littermates (Control; *n* = 31), ciguatoxin-induced cold allodynia (P-CTX-1, 5 nM; 15°C) is reduced in TRPA1^{-/-} (*n* = 14), but not in TRPM8^{-/-} (*n* = 7) or TRPV1^{-/-} (*n* = 10) animals, or after intraplantar treatment with the TRPM8 antagonist AMTB (100 μM). All data are presented as mean ± s.e.m. Statistical significance was determined using a one-way ANOVA with Dunnett's *post hoc* comparison; **P* < 0.05.

reports showing that A-fibres are devoid of TTXr Na_v1.8 (Akopian *et al*, 1996; Zimmermann *et al*, 2007). Ciguatoxin-induced A-fibre activity was suppressed by warming, while re-cooling (to cool temperatures or skin temperature) immediately reactivated action potential firing (Figure 5C). This effect was unaltered in TRPA1^{-/-} mice (Figure 5E). Residual cold sensitivity in sensory neurons, which cannot be

attributed to TRPA1 or TRPM8, has been described in the literature, although the molecular identity of the responsible cold transducer remains unknown to date (Bautista *et al*, 2007; Munns *et al*, 2007; Knowlton *et al*, 2010). Since A-fibres arise from large diameter DRG neurons that do not survive culture conditions well, such effects may have escaped detection in our cultured DRG neuron assays (Figures 2 and 3).

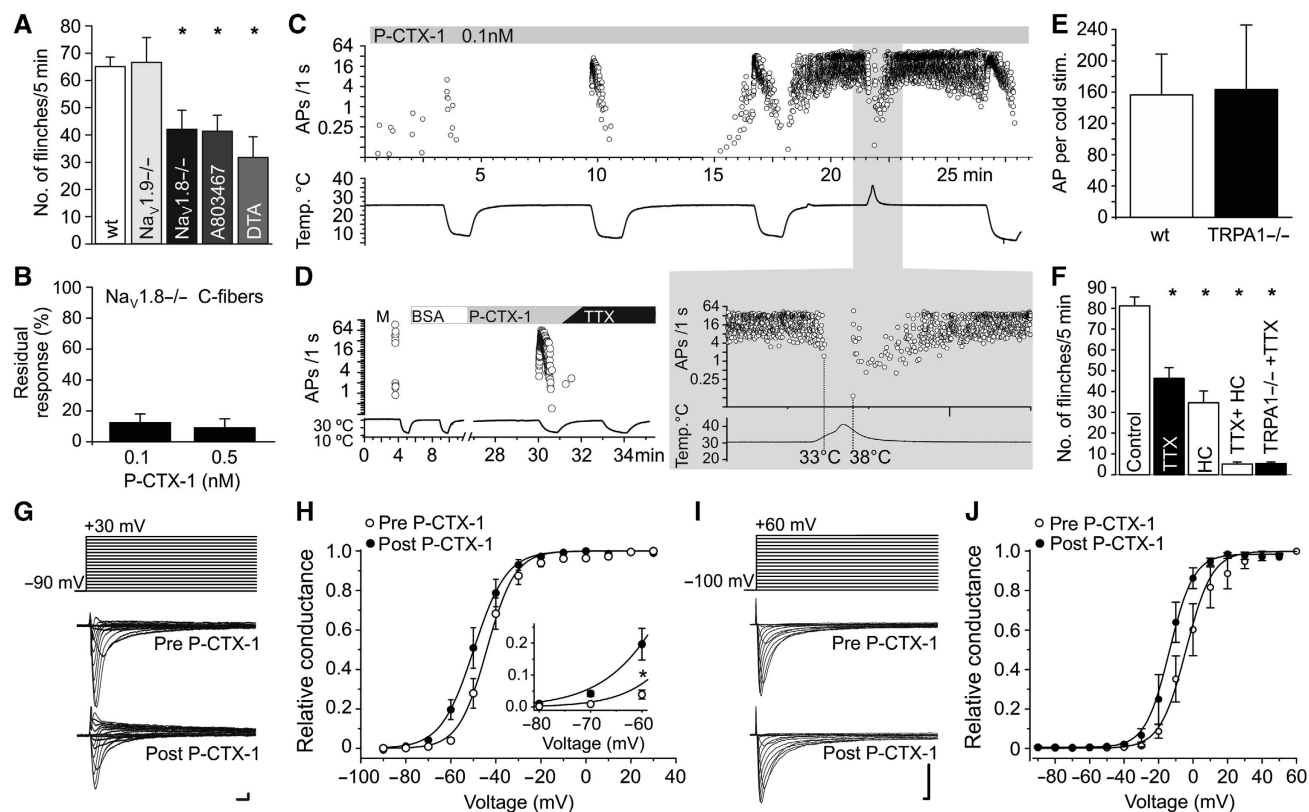


Figure 5 TTXr $\text{Na}_v1.8$ and TTXs sodium channels are effectors of ciguatoxin-induced cold allodynia. (A) Compared to *wt* littermates (Control; $n = 47$), ciguatoxin-induced cold allodynia (P-CTX-1, 5 nM; 15°C) appears unchanged in $\text{Na}_v1.9^{-/-}$ ($n = 12$), but markedly reduced in $\text{Na}_v1.8^{-/-}$ ($n = 16$) animals. This was confirmed using the $\text{Na}_v1.8$ blocker A803467 injected i.p. (10 μM in a volume of 40 μl ; $n = 11$) and in mice with diphtheria toxin-mediated ablation of $\text{Na}_v1.8$ -expressing nociceptors ($\text{Na}_v1.8$ -DTA; $n = 6$) animals. (B) P-CTX-1-induced ongoing activity is reduced by $> 85\%$ in C-fibers from skin-saphenous nerve preparations from $\text{Na}_v1.8$ -deficient mice. (C, D) Representative recording from a *wt* A-fibre. P-CTX-1 (0.1 nM) significantly increased activity of A-fibers in isolated mouse skin-saphenous nerve preparations. (C) Repeated cold stimulation of an A-fibre (C57BL/6, conduction velocity 11.9 m/s, 1.4 mN) after treatment with P-CTX-1 led to increasing action potential discharge until spontaneous activity occurred at 30°C . This activity was suppressed by heating (threshold temperature 33°C) and resumed upon cooling $< 38^\circ\text{C}$. (D) P-CTX-1 (0.1 nM) induced effects in A-fibers were entirely sensitive to TTX applied at 300 nM and (E) independent of TRPA1 (bars represent mean of two cold responses; *wt*: white bars, $n = 11$ and $\text{TRPA1}^{-/-}$: black bars, $n = 15$). (F) Compared to *wt* littermates (Control; $n = 13$), ciguatoxin-induced cold allodynia was significantly reduced by intraplantar injection of TTX (2 μM , $n = 13$) or the TRPA1 blocker HC030031 (100 μM ; $n = 6$). Combination of both compounds ($n = 6$) or application of TTX in TRPA1-deficient animals ($n = 5$) abolishes ciguatoxin-induced cold allodynia. (G) Representative TTXs current traces recorded from large-sized DRG neurons ($42.9 \pm 1.4 \mu\text{m}$). Upper lane: voltage protocol; middle: traces before and lower: traces after perfusion with P-CTX-1 (1 nM). (H) Effect of P-CTX-1 (1 nM) on the voltage-conduction relationship of TTXs channels measured in mouse DRG neurons ($n = 9$). (I) Representative recording of current traces recorded from ND7/23 cells heterologously expressing $\text{Na}_v1.8$. Upper lane: voltage protocol; middle: traces before and lower: traces after perfusion with P-CTX-1 (1 nM). (J) Effect of P-CTX-1 (1 nM) on the voltage-conduction relationship of $\text{Na}_v1.8$ heterologously expressed in ND7/23 cells ($n = 5$); scale bars in (G, I) represent 1 ms and 1 nA; all data are presented as mean \pm s.e.m.

This suggests that the residual cold allodynia observed in TRPA1-deficient mice arises from the effects of P-CTX-1 on these TTXs fibres. Indeed, the contribution of TTXs channels to ciguatoxin-induced cold allodynia was further confirmed in behavioural experiments, where i.pl. administration of TTX (2 μM) significantly decreased ciguatoxin-induced cold allodynia by 30% (Figure 5F). Furthermore, cold allodynia was completely abolished by simultaneous i.pl. injection of HC030031 and TTX, or in TRPA1 $^{-/-}$ mice treated with i.pl. TTX (Figure 5F).

To start to explain these results, we investigated the effect of P-CTX-1 on the biophysical properties of TTXs and TTXr Na_v in voltage-clamp recordings (Figure 5G–J). Consistent with previous reports (Strachan *et al*, 1999), P-CTX-1 shifted the voltage dependence of activation of TTXs channels at 23°C by $7.3 \pm 1.0 \text{ mV}$ to more negative potentials, inducing

significant channel activation at -60 mV (see insert in Figure 5G), a potential close to the supposed resting membrane potential of DRG neurons (Amir *et al*, 1999). Similarly, P-CTX-1 elicited a 10 mV hyperpolarizing shift of the voltage dependence of $\text{Na}_v1.8$ (Figure 5I) that persisted at cooler temperatures (Yamaoka *et al*, 2009).

In A-fibres, cold sensitization occurred at innocuous cool temperatures ($28\text{--}20^\circ\text{C}$), where only few TTXs channels are in a state of slow inactivation (Zimmermann *et al*, 2007). Thus, the shift in activation elicited by P-CTX-1 results in overactive TTXs channels that are able to fire at high rates during mild cooling. This effect of P-CTX-1 is presumably synergized by the effects of P-CTX-1 on voltage-gated potassium channels (Birinyi-Strachan *et al*, 2005) and the biophysical effects of cooling. Cooling decreases the activation threshold of the sodium currents, leads to an

increase in membrane resistance and results in depolarizing closure of background potassium channels (Griffin and Boulant, 1995; Maingret *et al*, 2000; Reid and Flonta, 2001; Viana *et al*, 2002; Zimmermann *et al*, 2007). These biophysical effects presumably are of major importance in nerve endings due to their high surface area to volume ratio. In contrast, a decrease in membrane resistance and opening of potassium channels during heating may short circuit the sodium current and opposes the ciguatoxin-induced increase in neuronal excitability (Figure 5C, inset), providing a biophysical explanation for the pain-relieving effects of warmth and the 'temperature reversal' reported in clinical ciguatera cases.

P-CTX-1 and cool temperatures synergistically activate TRPA1-expressing nociceptors to mediate the perception of burning pain

Our results from both behavioural experiments and single-fibre recordings clearly demonstrate a contribution of both TTXs and TTXr VGSCs, in addition to a major role of TRPA1-expressing C-fibres as mediators of ciguatoxin-induced cold allodynia. Thus, while TRPA1 has been established to be activated by temperatures in the noxious range, our results clearly demonstrate that TRPA1-expressing nociceptors are activated at higher temperatures in the presence of ciguatoxin. To explore the role of TRPA1 in temperature-induced nociception further and to analyse to which extent the central processing of cold stimuli and cold allodynia is affected by a lack of TRPA1, we used non-invasive functional MRI (fMRI) measurements (Figure 6A–G; Supplementary Figure 6). Here, changes in BOLD (Blood Oxygenation Level Dependent) signal were measured as a surrogate parameter for changes in neural activity (Hess *et al*, 2011) caused by repetitive cool stimulation (15°C) of the paw after ciguatoxin application. P-CTX-1 treatment elicited a marked increase in the cool stimulus-evoked BOLD signal, an effect which was blunted in TRPA1 $-/-$ animals (Figure 6A), consistent with the significant reduction in ciguatoxin-induced cold allodynia we observed in behavioural experiments on these knockout mice. Brain structures which showed differentially stronger activation by cool stimulation in *wt* compared to TRPA1 $-/-$ mice after P-CTX-1 injection included cerebral targets of the spino-mesencephalic and spino-reticular tract, the medial thalamus, ventral striatum, cingulum and periaqueductal grey (Figure 6), supporting our behavioural observation that TRPA1 crucially contributes to ciguatoxin-induced cold allodynia.

Surprisingly, we also observed differences in the central processing of the cold (15°C) stimulus under control conditions, where *wt* mice expressed stronger responses mainly in cortical areas in response to cooling of the paw (Supplementary Figure 6). Moreover, we found that the TRPA1 $-/-$ mice showed an altered kinetic of the hemodynamic response function (HRF) in response to cold stimuli, either with or without P-CTX-1 treatment (Supplementary Figure 6), providing the first evidence that the HRF can also be modulated by genetic influence. These results demonstrate that TRPA1 contributes not only to cold allodynia, but also that TRPA1-expressing fibres are activated at much higher temperatures than previously observed. TRPA1 is generally considered to be a sensor of noxious cold temperatures, with behavioural differences in knockout animals occurring at

temperatures close to freezing (Karashima *et al*, 2009). However, based on our results, previous behavioural studies in TRPA1 $-/-$ mice may have underestimated the contribution of TRPA1 to cold nociception, as small differences in perception may not lead to frank behavioural changes.

Discussion

Humans are able to detect a broad range of temperatures through activation of thermosensitive nerve endings in the skin. In recent years, significant advances have been made with the identification of several thermosensitive ion channels, in particular the TRP class of thermoreceptors that function as the molecular transducers of innocuous and noxious temperatures. Nevertheless, our understanding of the physiological and pathophysiological role of these channels remains incomplete and moreover, it remains unclear how temperature detection overlaps with the perception of pain. A particularly puzzling and poorly understood phenomenon is cold allodynia, where non-noxious and normally non-painful cool stimuli are perceived as painful. In this context, ciguatera is of particular interest as it is associated with the pathognomonic symptom of cold allodynia and thus may be useful to further dissect the pathways involved. Although it is known that ciguatoxin increases neuronal excitability through activation of VGSCs, the neuronal pathways leading to ciguatoxin-induced cold allodynia are unknown.

Peripheral administration of P-CTX-1 elicits cold allodynia

This study is the first to identify the sensory neuronal populations involved in mediating the symptomatology of ciguatera, and to elucidate the cellular and molecular basis of ciguatoxin-induced cold allodynia. The toxicokinetics of ciguatoxin are complex and likely contribute to the clinical presentation of ciguatera (Bottein *et al*, 2011). After oral administration in mice, ciguatoxin is rapidly absorbed from the gastrointestinal tract, where it exerts local action to elicit gastrointestinal symptoms such as diarrhoea and abdominal pain (Bottein *et al*, 2011). The clearance of ciguatoxin involves a bi-exponential elimination best fit using a two-compartment model. This probably occurs due to accumulation of P-CTX-1 in adipose tissue or even lipophilic neuronal membranes, which contributes to a long terminal elimination half-life of ~ 4 days. The slow elimination of P-CTX-1 likely contributes to the prolonged duration of neurological effects, and renal excretion of ciguatoxin may contribute to urinary symptoms such as dysuria, although the majority of ciguatoxin is excreted in the faeces. We postulate that the peripheral sensory effects of ciguatoxin after oral consumption arise from a direct excitatory action of the toxin on peripheral sensory neurons. In unpublished observations, intradermal administration of P-CTX-1 in humans elicits symptoms including cold allodynia, consistent with the symptomatology of ciguatera, providing direct support for our new animal model of cold allodynia. This mouse model reveals for the first time that altered excitability of peripheral sensory neurons is sufficient for the development of cold allodynia. The temperature dependence of allodynia observed in this mouse model was similar to the reported

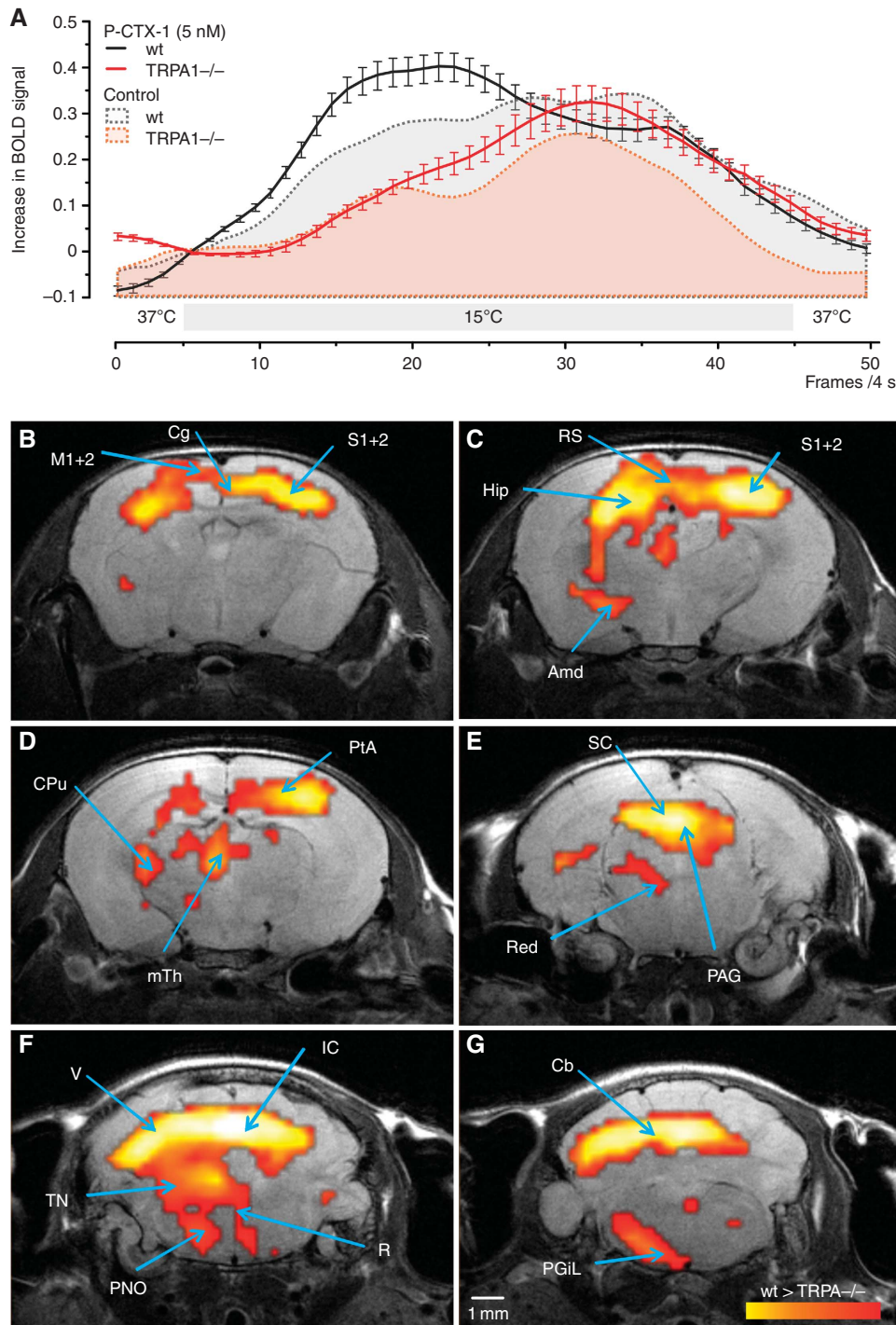


Figure 6 Cool temperatures and P-CTX-1 activate TRPA1-dependent nociceptive pathways resulting in the perception of burning pain. (A) Compared to *wt* animals (grey area under the curve), *TRPA1*^{-/-} mice (red area under the curve) showed an altered hemodynamic response function (HRF) in response to stimulation of the paw with 15°C after i.pl. injection of saline, but also in the presence of P-CTX-1 (black and red timelines). Changes in BOLD signal from *n* = 9–10 animals were averaged over six repetitive cold stimuli. Error bars represent s.e.m. (B–G) Second order statistical parameter maps showing differential brain activity (*wt* > *TRPA1*^{-/-}) assessed by BOLD-fMRI in response to cold stimulation following i.pl. P-CTX-1 treatment (5 nM i.pl.) in *wt* and *TRPA1*^{-/-} animals, superimposed on the corresponding anatomical image. The yellow-red scale indicates increased activity in *wt* compared to *TRPA1*^{-/-} animals. Arrows indicate regions with increased differential activity. For cold stimulation after i.pl. injection of P-CTX-1 (5 nM), (B) the somatosensory (S1/S2) cortex, the cingulate (Cg) cortex and the motor (M1/M2) cortex, (C) the retrosplenial cortex (Rs), hippocampus (Hip), amygdala (Amd), (D) striatum (CPu), parietal association cortex (PtA), medial thalamus (mTh), (E) superior colliculus (SC), red nucleus (Red), periaqueductal grey (PAG), (F) visual cortex (V), inferior colliculus (IC), raphe nucleus (R) tegmental nuclei (TN), pontine reticular nucleus (PNO) (G) cerebellum (Cb) and lateral paragigantocellular nucleus (PGIL) show significantly higher activity in *wt* than in *TRPA1*^{-/-} mice.

threshold of cold allodynia in human ciguatera patients (24–26°C) (Cameron and Capra, 1993). Interestingly, heat allodynia is neither observed clinically (Cameron and

Capra, 1993), nor was it observed in our animal model. The precise reasons for the lack of heat hyperalgesia remain to be determined; however, it is likely that differential

co-expression with CTX-sensitive Na_v and K_v channels contribute to this effect. In addition, mechanical allodynia is neither observed in ciguatera patients, nor was it apparent in our animal model. Thus, cold allodynia is the dominant thermal sensory abnormality present both clinically and in our animal model and is likely to be mediated by specific thermotransducer proteins.

TRPA1 is a critical determinant in ciguatoxin-induced cold allodynia

The involvement of two likely candidates, TRPM8 and TRPA1, in thermosensing is contentious. TRPM8 is activated by innocuous cool temperatures $<28^\circ\text{C}$, although activity is maintained in the noxious cold range ($<10^\circ\text{C}$) (McKemy *et al*, 2002; Peier *et al*, 2002). Accordingly, TRPM8 has been reported to be involved in temperature preference and environmental as well as noxious cold sensing (Peier *et al*, 2002; Bautista *et al*, 2007; Dhaka *et al*, 2007). In contrast, the cold receptor TRPA1 is thought to be activated by noxious cold temperatures in heterologous expression systems (Story *et al*, 2003; Karashima *et al*, 2009). However, a lack of cold-evoked TRPA1 responses, or only indirect activation through cold-induced Ca^{2+} release, has been reported by several groups (Jordt *et al*, 2004; Nagata *et al*, 2005; Zurborg *et al*, 2007). Similarly, differences in behaviour in TRPA1 $-/-$ animals were only reported at noxious temperatures or in pathological models of cold hypersensitivity, or not at all (Bautista *et al*, 2006; Karashima *et al*, 2009; del Camino *et al*, 2010; Gentry *et al*, 2010; Knowlton *et al*, 2010; Nassini *et al*, 2011). In the present study, we provide fMRI evidence that TRPA1 is activated by temperatures well above the noxious range and that TRPA1 is a critical determinant in ciguatoxin-induced cold allodynia. In cultured DRG neurons, Ca^{2+} responses to cooling, which appeared after P-CTX-1 treatment in previously cold-insensitive neurons, were completely dependent on TRPA1. In contrast, Ca^{2+} responses in cold-sensitive DRG neurons were neither significantly affected by P-CTX-1 nor affected in TRPA1-deficient mice (Figure 3). These cold responses are likely to be mediated through TRPM8, as both the temperature threshold of activation and the proportion of DRG neurons responding to cooling with increases in Ca^{2+} are in accordance with the literature values for TRPM8-mediated calcium increases (Bautista *et al*, 2007).

While some TRPM8-expressing neurons were activated by P-CTX-1, it is likely that these neurons are involved in ciguatoxin-induced symptoms other than cold allodynia, such as increased tear production (lachrymation) observed in rodents (Lewis and Sellin, 1993), a response that has recently been shown to depend on TRPM8 in mice (Parra *et al*, 2010). In contrast, studies in human ciguatera patients (Cameron and Capra, 1993) and intracutaneous injection of P-CTX-1 in humans (unpublished observations) have revealed that temperature discrimination and cool sensitivity, which are painless sensations mediated through TRPM8 (Bautista *et al*, 2007; Parra *et al*, 2010), are not altered by P-CTX-1. Given the main effect of P-CTX-1 is the emergence of the sensation of pain in response to mild cooling, it appears that the cold sensing TRPA1 rather than TRPM8 couples to pain sensing centrally. This was confirmed in behavioural experiments, where ciguatoxin-induced cold

allodynia was significantly decreased in TRPA1 $-/-$ mice, but not affected in TRPM8 $-/-$ animals.

TRPA1 contributes to cold sensing at higher temperatures than previously recognized

Lastly, we demonstrated altered central processing of cold allodynia after P-CTX-1 treatment in TRPA1 $-/-$ versus *wt* mice. In the process, we also revealed for the first time that the TRPA1-dependent cold nociceptive pathway is activated at temperatures well above the noxious cold range and that this signal is processed in the brain well before it results in measurable aversive behaviour in the noxious cold range (e.g., $<10^\circ\text{C}$), suggesting it may play a broader role in protecting the body from damaging cold than previously recognized. TRPA1-mediated effects were observed in brain areas associated with emotion, pain and cold processing, in particular the amygdala, cingulate cortex, and the S1 and S2 somatosensory cortices, illustrating subtle differences in cool perception in TRPA1 $-/-$ mice. Furthermore, C-fibres share input to spinal laminae I-III and build projections into the spino-mesencephalic tract, an area which appeared in the fMRI experiment among those with differentially stronger activation during cold allodynia in *wt* mice. Interestingly, previous fMRI studies in human subjects found analogous brain areas to be activated during heat and cold hypersensitivity (Lorenz *et al*, 2002; Seifert and Maihöfner, 2007), including projections within the spino-mesencephalic tract, corroborating an important role of TRPA1 in cold sensing in the non-noxious temperature range. This was also observed in behavioural experiments utilizing pharmacological modulators administered by the i.pl. route, and are strongly supported by *ex-vivo* findings in the isolated skin-nerve preparation. Thus, these findings provide clear evidence for a role of TRPA1 in cold sensing at higher temperatures than previously recognized.

This study shows that i.pl. injection of P-CTX-1 elicits cold, but no heat or mechanical allodynia. While TRPA1 has been implicated as a mechanosensor, it is not absolutely required for mechanical sensitivity of afferent nerve terminals *per se*, as mechanically sensitive cutaneous fibres are present in normal numbers in TRPA1-deficient mice and deficits of TRPA1-deficient mice to mechanical force were only observed in response to intense mechanical stimulation (Kwan *et al*, 2009). However, slowly adapting low-threshold A β mechanoreceptors from TRPA1-deficient mice have been shown to have reduced action potential firing, suggesting a role of TRPA1 in mechanosensation in these fibres. It is plausible that TRPA1-mediated mechanosensation in these fibres contributes to ciguatoxin-induced sensory disturbances other than mechanical allodynia, such as the tingling and pricking sensations which are commonly described by ciguatera victims, but which are difficult to assess in this murine model.

Ciguatera is a special form of acquired channelopathy

Despite the dominant role of TRPA1 in ciguatoxin-induced cold allodynia, this effect does not appear to be mediated by a direct action of P-CTX-1 on thermosensitive TRP channels. Instead, TRPA1-mediated cold allodynia occurs indirectly through changes in neuronal excitability and membrane potential elicited by P-CTX-1 (Carr *et al*, 2002). P-CTX-1 activates Na_v and inhibits K_v channels, resulting in

sustained membrane depolarization of several mV (Strachan *et al*, 1999; Birinyi-Strachan *et al*, 2005). Under these conditions, a cooling-induced change in the voltage dependence of TRPA1 activation appears sufficient for TRPA1-mediated responses to reach the threshold for action potential generation and to signal burning pain at innocuous cool temperatures. Indeed, depolarization-mediated activation of thermo-TRP channels has been reported recently in heterologous expression systems, further supporting our findings. The fact that voltage-dependent gating is tightly linked to temperature sensing in TRPs is not a new concept (Voets *et al*, 2004), but in the case of ciguatoxin it becomes pathologic. Differences in resting membrane potential could also provide an explanation for the observation that TRPA1-mediated cold responses can be elicited in heterologous expression systems with relatively positive membrane potentials (Chemin *et al*, 2000; Kim *et al*, 2004), but not in DRG cell somata with their relatively hyperpolarized resting membrane potential (Reid, 2005; Zurborg *et al*, 2007; Caspani and Heppenstall, 2009). Thus, the ciguatoxin-mediated increase in the excitability of a subset of neurons—in the absence of direct effects on thermo-TRP channels—is sufficient to elicit profound sensitization to cooling. This increase in excitability is driven in part by Na_v1.8, consistent with its role in cold pain and previous reports of effects of ciguatoxins on Na_v1.8 (Strachan *et al*, 1999; Yamaoka *et al*, 2009). However, a significant contribution of TTXs channels to ciguatoxin-mediated cold sensitization was also observed. In contrast to noxious cold temperatures (<10°C), where TTXs channels have entered into a state of slow inactivation (Zimmermann *et al*, 2007), these channels contribute to cold allodynia at innocuous cool temperatures, where they are still able to fire at high rates. This effect is potentiated by the closure of temperature-sensitive potassium channels and the biophysical effects of cooling, which decrease the activation threshold of the sodium currents, lead to an increase in membrane resistance and result in depolarizing closure of background potassium channels (Griffin and Boulant, 1995; Maingret *et al*, 2000; Reid and Flonta, 2001; Viana *et al*, 2002; Zimmermann *et al*, 2007). Taken together, modulation of biophysical membrane properties by cooling in combination with altered membrane potential through Na_v activation by P-CTX-1 can be sufficient to elicit action potential bursts and strong and long-lasting spontaneous activity consistent with the prolonged neurological effects of P-CTX-1 observed in ciguatera victims. Thus, while it has been established that both Na_v1.8 and TRPA1 are required for noxious cold sensing (Zimmermann *et al*, 2007; Karashima *et al*, 2009), our findings show that TRPA1-dependent nociception is activated at innocuous cold temperatures under circumstances where activation of Na_v increases membrane excitability, as is the case for ciguatoxin and potentially in neuropathic pain states associated with cold allodynia.

In conclusion, ciguatera can be described as a special form of acquired channelopathy that provides unique insight into the mechanisms of cold transduction and sensitization. P-CTX-1 elicits striking peripheral activation in C-fibres as well as *de-novo* sensitization and activation in A-fibres, with P-CTX-1 preferentially targeting peptidergic, IB4-negative TRPA1-expressing nociceptors. While P-CTX-1 does not directly activate thermo-TRP channels, TRPA1 is crucial to the development of ciguatoxin-induced cold allodynia, where

membrane depolarization through activation of sodium channels in TRPA1-containing neurons leads to peripheral sensitization and consequently to activation of a specific subset of brain structures relevant for allodynia. In addition to Na_v activation through P-CTX-1, cold temperatures further enhance neuronal excitability by increasing membrane resistance to produce the pathognomonic symptom of cold allodynia. The recent report that TRPA1-expressing fibres also mediate itch (Wilson *et al*, 2011) may explain the intense pruritus observed clinically, and further supports the notion that TRPA1-expressing nociceptors are particularly susceptible to the effects of ciguatoxin.

Materials and methods

Materials

P-CTX-1 (>90% purity) was isolated from moray eel (*Gymnothorax javanicus*) liver as previously described (Lewis *et al*, 1991), stored as a concentrated stock in 50% methanol/50% H₂O and routinely diluted in the presence of 0.1–0.3% bovine serum albumin (BSA) to avoid loss to plastic. All other reagents were from Sigma-Aldrich (Castle Hill, NSW, Australia or Taufkirchen, Germany) unless otherwise stated.

Ethics for animal experiments

The protocol for *in-vivo* experiments in animals was reviewed by the local animal ethics committee (University of Erlangen) and approved by the local district government. At the University of Queensland, ethical approval for experiments involving animals was obtained from the local animal ethics committee. Experiments involving animals were conducted in accordance with the Animal Care and Protection Act Qld (2002), the *Australian Code of Practice for the Care and Use of Animals for Scientific Purposes*, 7th edition (2004) and the *International Association for the Study of Pain Guidelines for the Use of Animals in Research*.

Origin of mice

We used adult male C57BL/6J mice, TRPA1^{-/-} (D Corey, Harvard Medical School, Boston, MA, USA; backcrossed for nine generations on C57BL/6), TRPV1^{-/-} (J Davis, formerly GlaxoSmithKline, Harlow, UK; congenic to C57BL/6), TRPM8^{-/-} (A Patapoutian; backcrossed for five generations on C57BL/6 background), Na_v1.8^{-/-}, Na_v1.9^{-/-}, Na_v1.8-DTA mice (John N Wood, University College London, London, UK; congenic to C57BL/6 or backcrossed for at least six generations on the C57BL/6 background, respectively) knockout mice and their age-matched litter controls were used or matched to C57BL/6J when congenic. All animals were genotyped using previously reported primers.

Animal model of ciguatoxin-evoked nocifensive behaviour and cold allodynia

To assess ciguatoxin-evoked effects in *wt* C57BL/6 and in age-matched TRPV1^{-/-}, TRPA1^{-/-} and TRPM8^{-/-} mice, a single dose of P-CTX-1 was administered by subcutaneous injection to the hind paw (i.pl.) and nocifensive behaviour was rated by a blinded observer. P-CTX-1 was prepared in concentrations of 0.01–10 nM (final dose of 0.5–50 pg/paw) in sterile Ringer's solution and injected i.pl. in a volume of 40 µl under light diethyl ether, methoxyflurane or isoflurane anaesthesia. To assess the effects of pharmacological modulators on the development of spontaneous pain and cold allodynia, compounds were either administered by i.p. injection 30 min prior to i.pl. injection of P-CTX-1 (HC030031, 100 mg/kg i.p.) or were co-administered with P-CTX-1 by i.pl. injection as appropriately concentrated solutions (HC030031, 100 µM; TTX, 2 µM; A803467, 10 µM).

After a brief recovery period, spontaneous pain was rated at room temperature by counting the number of paw shakes, lifts, licks or flinches over a 5-min period. To assess heat and cold allodynia in ciguatoxin-treated animals, mice were placed on a temperature-controlled Peltier plate (Ugo Basile, Comerio, Italy or a custom-designed Peltier-based plate with components purchased from Melcor, Trenton, NJ, USA) once spontaneous pain behaviour

subsided to <10 counts/5 min and the number of paw shakes, lifts, licks or flinches was quantified over a 5-min period.

To assess contribution of Na_v and thermo-TRP channels to the development of ciguatoxin-induced cold allodynia, nocifensive behaviour in response to i.p.l. injection of 5 nM P-CTX-1 was determined over a 5-min period at 15°C, 60–90 min after treatment with P-CTX-1.

No systemic effects, including no diarrhoea, ataxia, altered gait or motor paralysis were apparent in any mice and all animals completely recovered within several hours. In addition, no sustained hind paw favouring, inflammation, swelling or ulceration of the ciguatoxin-injected paw was visible. Injection of equal volumes of Ringer's solution did not elicit any nocifensive behaviour (Figure 1B).

DRG cell culture

DRGs were isolated and cultured as previously described (Zimmermann *et al*, 2007). In brief, DRGs from T1-L6 were isolated from adult male Wistar rats, male C57/BL6 mice, male $\text{Na}_v1.8$ $-/-$ mice or male TRPA1 $-/-$ mice euthanized by CO_2 inhalation and collected in DMEM supplemented with 50 $\mu\text{g}/\text{ml}$ gentamicin (Sigma), 100 U/ml penicillin, 100 $\mu\text{g}/\text{ml}$ streptomycin and 0.25 $\mu\text{g}/\text{ml}$ amphotericin B (Invitrogen). DRGs were then incubated for 30 min at 37°C and 5% CO_2 in dissociation media containing 1 mg/ml collagenase (Sigma) and 0.1 mg/ml protease (Sigma). After three wash steps, cells were triturated through a flame-polished glass Pasteur pipette and cultured for 24 h in TNB 100 solution supplemented by TNB 100 lipid-protein complex, 1 nM NGF, 100 $\mu\text{g}/\text{ml}$ streptomycin and penicillin (all from Biochrom, Berlin, Germany) and 200 $\mu\text{g}/\text{ml}$ glutamine (Invitrogen, Carlsbad, USA) or Neurobasal medium supplemented with B27, 1 nM NGF and 100 μM glutamine (all from Invitrogen, Mulgrave, VIC, Australia) for high content imaging.

High content imaging and immunochemical characterization of ciguatoxin-sensitive DRG neurons

Mouse DRG neurons were cultured on PDL-coated 96-well half area imaging plates (Corning) for 24 h and loaded with 5 μM Fura-2 for 30 min at 37°C. After two washes with physiological salt solution (PSS; composition: NaCl 140 mM, glucose 11.5 mM, KCl 5.9 mM, MgCl_2 1.4 mM, NaH_2PO_4 1.2 mM, NaHCO_3 5 mM, CaCl_2 1.8 mM, HEPES 10 mM), Ca^{2+} responses to stimulation with P-CTX-1 (1 nM) or AITC (100 μM) were measured using the high content imager BD Pathway 855 (BD Biosciences, San Jose, CA, USA) for 60 s with a Hamamatsu Orca ER cooled CCD camera and $\times 10$ objective at 22°C. Cells were then fixed with Histochoice (Amresco, Solon, OH, USA) for 1 h, blocked with 0.3% BSA/0.1% gelatin in PBS at room temperature for 30 min, followed by staining with DAPI (1 $\mu\text{g}/\text{ml}$) and the primary antibodies characterized in Supplementary Table S1 for 1 h.

In addition, for visualization of neuron-specific β 3-tubulin, cultures were stained with mouse anti- β 3 tubulin antibody (TUJ1, R&D Systems, Minneapolis, MN, USA, 1:1000) and to verify specificity of the rabbit TRPA1 antibody, neurons were additionally stained with mouse monoclonal anti-TRPA1 (Sigma, WH0008989M3, 1:1000). After three washes with PBS, DRG cultures were then incubated for 1 h with the following secondary antibodies as appropriate: anti-rabbit Alexa Fluor[®] 488 (Invitrogen, 1:1000); anti-sheep Alexa Fluor[®] 647 (Invitrogen, 1:1000); anti-guinea pig Alexa Fluor[®] 647 (Invitrogen, 1:1000); anti-mouse Alexa Fluor[®] 488. DRG cultures were washed three times with PBS and immunofluorescence visualized using the BD Pathway 855 with $\times 10$ objective.

ROIs corresponding to antibody-positive DRG neurons were identified and Ca^{2+} responses, expressed as $\Delta R/R$, were plotted using GraphPad Prism 4. Only cells with clearly defined ROI corresponding to single DRG neurons were used for analysis. DRG neurons were classified as responders if stimulation with 1 nM P-CTX-1 elicited a $\Delta R/R$ increase of at least 0.15 over 60 s ($n = 771/1524$ neurons classified as responders).

Pharmacological characterization of ciguatoxin-sensitive DRG neurons

Rat DRG neurons were plated on PDL-coated glass coverslips and after 24 h culture loaded with 5 μM Fura-2 and 0.02% pluronic F-127 for 30 min at 37°C and 5% CO_2 . After a brief wash to allow for deesterification, coverslips were transferred to the recording cham-

ber of an Olympus IX71 inverse microscope with an $\times 20$ objective and Ca^{2+} responses were measured at 22°C. Fura-2 was excited at 340 and 380 nm with a Lambda DG-4 (Sutter Instruments Co.). Images were exposed for 100 ms and acquired at a rate of 3 Hz with a CCD camera (Orca-ER; Hamamatsu Photonics). Data were recorded and further analysed using Metamorph (MDS Analytical Technologies). Background was subtracted before calculation of ratios. After a baseline read with extracellular solution (ECS, composition: NaCl 145 mM, KCl 5 mM, CaCl_2 1.25 mM, MgCl_2 1 mM, glucose 10 mM, HEPES 10 mM), DRG neurons were stimulated with 1 nM P-CTX-1, followed by perfusion with 300 nM TTX. To identify TRPA1-expressing neurons, DRGs were stimulated with AITC (25 μM), while stimulation with 50 mM KCl was used to identify viable neurons. AITC-sensitive neurons were defined as cells exhibiting an increase of the ratio R of at least 15% over baseline fluorescence upon stimulation with AITC; TTXs cells were defined as cells exhibiting a decrease in intracellular Ca^{2+} of at least 50%. Ca^{2+} responses were presented as the fluorescence ratio R F340/380 or converted to intracellular Ca^{2+} concentration after calibration of Fura-2 fluorescence, using an experimentally determined K_d of 135 nM and a value of 0.2 and 2.6 for R_0 and R_1 , respectively.

P-CTX-1 effects on cold-induced Ca^{2+} responses in DRG neurons

Dissociated DRG neurons from *wt* and TRPA1 $-/-$ mice were plated on PDL-coated glass coverslips as described above. Recordings were performed on an Olympus IX71 inverse microscope with a $\times 20$ objective and Ca^{2+} responses were measured at 35°C. Fura-2 was excited at 340 and 380 nm with a Polychrome V monochromator (Till Photonics). Images were exposed for 200 μs and acquired at a rate of 1 Hz with a 12-bit CCD camera (Imago Sensicam QE, Till Photonics). Data were recorded and further analysed using TILLvisION 4.0.1.3 software (Till Photonics). To assess Ca^{2+} responses to cold stimulation and at different temperatures, a system for fast superfusion of the cultured cells was used (Dittert *et al*, 2006). Experimental solutions were driven by gravity from six barrels through electronically controlled valves into a manifold that consisted of fused silica tubes connected to an outlet glass capillary. The temperature of the solutions was preconditioned in a heat exchanger by a miniature Peltier device. The final temperature was adjusted by densely coiled copper wire, which wrapped the lower part of the capillary. The temperature was measured by a miniature thermocouple inserted into the outlet capillary near to its orifice. After the baseline was established at 35°C, DRG neurons were cooled in a ramp-shaped manner to 15°C over a period of 180 s, followed by heating back to 35°C within 1 s. After 60 s, 1 nM P-CTX-1 was applied for 360 s, during which a second cold stimulus was delivered. For quantitative comparison of cold sensitization, the maximum increase in intracellular Calcium after cold stimulation, relative to the 10 baseline reads prior to the cold stimulus, was determined for control and ciguatoxin-treated cold responses. Neurons responding to the control cold response with an increase in intracellular calcium of at least 20 nM were classified as cold sensitive (34/204 neurons from *wt* and 28/406 neurons from TRPA1 $-/-$ mice), while neurons with an increase in $[\text{Ca}^{2+}]$ of <20 nM were classified as cold insensitive. Cold sensitization was defined as cold responses from previously cold-insensitive neurons that were at least five times larger after treatment with P-CTX-1 compared to control (67/170 neurons sensitized to cold in *wt* neurons and 25/378 sensitized to cold in TRPA1 $-/-$ neurons).

Cell culture and transfection procedures

Cos-1, HEK293 and ND7/23 cells (all from American Tissue Culture Collection, Manassas, VA, USA) were routinely maintained in DMEM containing 10% fetal bovine serum, 2 mM L-glutamine, pyridoxine and 110 mg/ml sodium pyruvate. Cells were split every 3–6 days in a ratio of 1:5 using 0.25% trypsin/EDTA. Cells were plated on T75 tissue culture flasks (Nunc) 24 h prior to transfection and transfected with plasmid DNA of hTRPV1 (J Davis, formerly GlaxoSmithKline, Harlow, UK), mTRPA1 (A Patapoutian, The Scripps Research Institute, La Jolla, CA, USA), $\text{rNa}_v1.8$ (C Nau, Department of Anesthesiology, Friedrich-Alexander-University Erlangen-Nuremberg, Erlangen, Germany), hTRPA1 (OriGene Technologies, Rockville, MD, USA) and $\text{hNa}_v1.7$ (N Klugbauer and

F Hofmann, Technische Universität Munich, Germany) using Fugene (Roche) or Nanofectin (Paa, Austria) according to manufacturer's instructions. Twenty-four hours after transfection, cells were plated on 96-well plates, 384-well plates or glass coverslips as required and used 24 h after plating.

Electrophysiological recordings from skin nerve preparations

The effects of P-CTX-1 on C- and A-fibres were assessed using single fibre recordings from isolated rat and murine skin-saphenous nerve preparations as previously described (Zimmermann *et al*, 2009).

The hairy skin of the dorsal hind paw and lower leg of male adult C57BL/6, TRPA1^{-/-}, Na_v1.8^{-/-} mice was removed together with the saphenous nerve, secured to the bottom of an organ chamber with the epithelial side facing down and continuously perfused with carbogenated SIF. Single A- and C-fibres were isolated from split single fibres of the desheathed saphenous nerve placed in a separate recording chamber under paraffin oil immersion. The receptive fields of the single fibres were identified using mechanical probing. For classification of fibres, the conduction velocity was determined by electrical stimulation of the receptive field with a concentric bipolar Platinum/Iridium steel microelectrode and mechanical sensitivity was assessed using a customized set of von Frey filaments.

The single fibre receptive fields were then isolated using a thin-walled glass ring (volume 500 µl) and continuously perfused at a rate of 10 ml/min for temperature control and superfusion with P-CTX-1 and TTX. In contrast to previous studies, the fibres were not subjected to heat stimulation in order to avoid induction of ongoing activity. This entailed classification of the fibres in two subtypes, CM and CMC. Since only very few CMC fibres were encountered the present results only summarize cold-insensitive CM-fibres. The cold stimulus (60 s) was applied using a counter-current heat exchange application system as previously described (Zimmermann *et al*, 2009). DAPSYS V7 (<http://www.dapsys.net>) was used to record and analyse the data.

Patch-clamp recordings

Effects of P-CTX-1 on the voltage dependence of activation were assessed in DRG neurons from Na_v1.8^{-/-} mice to eliminate the major TTXr component.

Whole-cell voltage-clamp recordings were performed with an EPC-10USB amplifier operated by PatchMaster software (HEKA Electronics, Lambrecht/Pfalz, Germany), using fire polished 1–1.5 MΩ borosilicate glass electrodes (Biomedical Instruments, Jena, Germany) containing (in mM): 140 CsF, 2 NaCl, 1 EGTA, 10 HEPES and 5 TEA-Cl; 308 mOsmol (pH 7.4, adjusted with CsOH), and the extracellular bath contained (in mM): 10 NaCl, 105 Cholin Cl, 3 KCl, 1 MgCl₂, 1 CaCl₂, 20 TEA-Cl, 0.1 CdCl₂, 10 glucose, 10 HEPES; 310 mOsmol (pH 7.4, adjusted with NaOH). For patch-clamp recordings of rNa_v1.8 in ND7/23 cells, the pipette solution contained (in mM): 140 CsF, 10 NaCl, 1 EGTA, 10 HEPES and 5 TEA-Cl; 308 mOsmol (pH 7.4, adjusted with CsOH) and the extracellular bath contained (in mM): 140 NaCl, 3 KCl, 1 MgCl₂, 1 CaCl₂, 20 TEA-Cl, 0.1 CdCl₂, 10 glucose, 10 HEPES; 326 mOsmol (pH 7.4, adjusted with NaOH). For current-clamp recordings of cultured DRGs, the pipette solution contained (in mM): 135 K-Gluconate, 4 NaCl, 3 MgCl₂, 0.3 Na-GTP, 2 Na₂-ATP, 5 EGTA, 5 HEPES; 280 mOsmol (pH 7.25, adjusted with KOH). All recordings were conducted at room temperature (~21 °C). Approximately 5 min after establishing cell access, voltage dependence of activation was assessed using 100 ms step depolarizations from a holding potential of -90 mV or -100, respectively. Between each voltage step ($\Delta V = 10$ mV, ranging from -90 to +30 mV, or from -90 to +60 mV, respectively) cells were held at V_{hold} for 5 s. Conductances were calculated from peak currents and normalized conductances were fitted using a Boltzmann equation using OriginPro 8.1 (OriginLab Corp., Northampton, MA, USA).

FLIPR Ca²⁺ Assays

To assess Ca²⁺ responses using the FLIPR^{TETRA} (Molecular Devices, Sunnyvale, CA, USA) plate reader, cells were plated at a density of 50 000 cells/well on 96-well black-walled imaging plates (Corning) or a density of 15 000 cells/well on 384-well black-walled imaging plates (Corning) 24 h prior to the assay. Cells were loaded with 5 µM Fluo-4 AM (Invitrogen) in PSS/0.3% BSA for 30 min at 37 °C and 5% CO₂, washed twice with PSS and transferred the recording chamber of the FLIPR^{TETRA}. Ca²⁺ responses were measured using a cooled

CCD camera (excitation, 470–495 nm; emission, 515–575 nm), with camera gain and intensity adjusted to yield a baseline fluorescence of 1000 arbitrary fluorescence units (AFUs). A two-addition protocol was used, consisting of 10 baseline fluorescence reads, addition of antagonists or P-CTX-1 with fluorescence reads every second for 300 s, followed by addition of agonists and a further 300 fluorescence reads in 1 s intervals. Raw fluorescence data were converted to $\Delta F/F$ values as described below.

fMRI in mice

Wt ($n = 9$) and TRPA1^{-/-} ($n = 10$) male mice were anaesthetized with isoflurane and placed on a cradle inside the MR scanner (Bruker BioSpec 47/40; 200 mT/m) with a free bore of 40 cm, equipped with an actively RF-decoupled coil system and a 4-channel head array coil under careful physiological monitoring (respiration, temperature). The temperature of the ciguatoxin-treated or saline-treated paw was controlled by contact using a miniature peltier device (6 mm² contact surface). In general, the temperature of the hind paw was kept at 35 °C, and, during six repetitive stimulations, cooled down to 15 °C for 120 s each (presented at 8 min intervals). The Peltier temperature was remote controlled using custom-made software as previously described (Neely *et al*, 2010). In short, a set of 750 functional EPI images were acquired with two times k-space averaging resulting in a TR of 4000 ms and a total measuring time of 50 min. Finally, 22 corresponding anatomical T2 reference images (field of view 15 × 15 mm, matrix 256 × 128, TR = 2000 ms, slice thickness 0.5 mm, TE_{eff} = 56 ms, RARE) were assembled. Functional analysis was performed using Brain Voyager QX and our custom-designed software, MagNan (Knabl *et al*, 2008). In brief, the following preprocessing was performed: Motion correction algorithm as implemented in BrainVoyager was applied (trilinear interpolation, motion detected always below 1 pixel). Slice time correction was performed with a Cubic Spline, followed by a high pass temporal filtering (nine cycles) and a 2D Gaussian smoothing of the data (FWHM kernel: 2 pixel, in-plane direction). Next, a single contrast-based GLM analysis (cold stimulus) for each animal was calculated. To detect significantly activated voxels, statistical parametric maps (SPMs) of these contrasts were generated for individual animals and FDR thresholded ($q = 0.05$, two-sided). Different groups of significantly activated voxels ($n > 4$) were labelled belonging to certain brain structures based on the mouse atlas from Paxinos (second edition). After registering the individual SPM's based on the manual segmented brains by a 12 degree affine transformation scheme they were averaged over all animals per group. Next, the resulting group average TRPA1^{-/-} map was subtracted from the *wt* map in order to reveal brain areas expressing higher BOLD signals in *wt* compared to TRPA1^{-/-} mice: these are the areas which are expected to be relevant for cold allodynia. Moreover, in a second, independent approach we characterized all structures of our pain matrix mouse atlas (Neely *et al*, 2010) by their temporal behaviour over the six stimulus repetitions. First, we calculated the group average BOLD peak response per repetition and brain structure based on the stimulus-specific GLM predictor. Next, these amplitudes of each brain structure were fitted by a linear model. All structures with a slope greater than 0.1 and an r^2 greater than 0.5 were assumed to be directly coupled to the increasing sensitization observed in response to consecutive cold stimuli as demonstrated in Figure 6 and Supplementary Figure 6.

Data analysis

Fluorescence values from Ca²⁺ imaging experiments were converted to $\Delta R/R$ (Fura-2) or $\Delta F/F$ (Fluo-4) values by subtracting baseline fluorescence readings from subsequent values and normalizing to baseline fluorescence as previously described (Minta *et al*, 1989). For concentration-response curves, maximum values from the response after addition of agonist were plotted against agonist concentration and a 4-parameter logistic Hill equation was fitted to the data using GraphPad Prism Version 4.00 (San Diego, CA, USA).

Statistical analysis

Statistical significance was defined as $P < 0.05$ and was determined using paired or unpaired Student's *t*-tests and one-way ANOVA analysis with Dunnett's post test as indicated. Statistical analysis was performed using GraphPad Prism Version 4.00 or Origin soft-

ware (OriginLab Corp., Northampton, USA) and SPSS 10.0 (SPSS Inc., USA).

Supplementary data

Supplementary data are available at *The EMBO Journal* Online (<http://www.embojournal.org>).

Acknowledgements

We would like to thank Iwona Izydorzyk and Jana Schramm for expert technical assistance, Mark Baker for insightful discussions and David Clapham for helpful comments on the manuscript and for financial support. Funding for this project was obtained through the Australian Research Council ARC LIEF grants for the BD Pathway 855 and FLIPR^{TETRA}, a National Health and Medical Research Council Fellowship and Program Grant (R.J.L.), a National Health and Medical Research Council Postdoctoral Fellowship (IV), an International Association for the Study of Pain Early Career

Research Grant (IV and KZ) and the Go8 Australia-Germany Joint Research Co-operation Scheme (IV and KZ). Additional support was obtained from the German Research Council (DFG): LA2740-2/1 (AL), Zi1172/1-1 (KZ), Re704/2-1 and KFO130/TP7 (PWR), 661/TP4 (AH); the Federal Ministry of Education and Research (BMBF): 01EM0514, 01GQ0731, 0314102 (AH); the Dr Ernst und Anita Bauer-Foundation (SS) and the STAEDTLER Foundation (KZ, PWR).

Author contributions: IV, RH, SS, AS, LC and KZ contributed to animal experiments; AH, MS and KZ performed fMRI experiments; IV, FT, AL, SS, MEb, MEh and KZ performed *in-vitro* experiments and/or data analysis; IV and KZ wrote the manuscript; and PC, JW, VV, PWR and RL provided intellectual guidance and financial support.

Conflict of interest

The authors declare that they have no conflict of interest.

References

- Abrahamsen B, Zhao J, Asante CO, Cendan CM, Marsh S, Martinez-Barbera JP, Nassar MA, Dickenson AH, Wood JN (2008) The cell and molecular basis of mechanical, cold, and inflammatory pain. *Science* **321**: 702–705
- Akopian AN, Sivilotti L, Wood JN (1996) A tetrodotoxin-resistant voltage-gated sodium channel expressed by sensory neurons. *Nature* **379**: 257–262
- Amaya F, Wang H, Costigan M, Allchorne AJ, Hatcher JP, Egerton J, Stean T, Morisset V, Grose D, Gunthorpe MJ, Chessell IP, Tate S, Green PJ, Woolf CJ (2006) The voltage-gated sodium channel Na(v)1.9 is an effector of peripheral inflammatory pain hypersensitivity. *J Neurosci* **26**: 12852–12860
- Amir R, Michaelis M, Devor M (1999) Membrane potential oscillations in dorsal root ganglion neurons: role in normal electrogenesis and neuropathic pain. *J Neurosci* **19**: 8589–8596
- Bagnis R, Kuberski T, Laugier S (1979) Clinical observations on 3,009 cases of ciguatera (fish poisoning) in the South Pacific. *Am J Trop Med Hyg* **28**: 1067–1073
- Bautista DM, Jordt SE, Nikai T, Tsuruda PR, Read AJ, Poblete J, Yamoah EN, Basbaum AI, Julius D (2006) TRPA1 mediates the inflammatory actions of environmental irritants and proalgesic agents. *Cell* **124**: 1269–1282
- Bautista DM, Siemens J, Glazer JM, Tsuruda PR, Basbaum AI, Stucky CL, Jordt SE, Julius D (2007) The menthol receptor TRPM8 is the principal detector of environmental cold. *Nature* **448**: 204–208
- Beaglehole JC (ed) (1961) *The Journals of Captain James Cook on His Voyages of Discovery: The Voyage of the Resolution and Adventure 1772–1775*, pp 469–470. Cambridge, England: Cambridge University Press
- Birinyi-Strachan LC, Gunning SJ, Lewis RJ, Nicholson GM (2005) Block of voltage-gated potassium channels by Pacific ciguatoxin-1 contributes to increased neuronal excitability in rat sensory neurons. *Toxicol Appl Pharmacol* **204**: 175–186
- Bottein MY, Wang Z, Ramsdell JS (2011) Toxicokinetics of the ciguatoxin P-CTX-1 in rats after intraperitoneal or oral administration. *Toxicology* **284**: 1–6
- Cameron J, Capra MF (1993) The basis of the paradoxical disturbance of temperature perception in ciguatera poisoning. *J Toxicol Clin Toxicol* **31**: 571–579
- Carr RW, Pianova S, Brock JA (2002) The effects of polarizing current on nerve terminal impulses recorded from polymodal and cold receptors in the guinea-pig cornea. *J Gen Physiol* **120**: 395–405
- Caspani O, Heppenstall PA (2009) TRPA1 and cold transduction: an unresolved issue? *J Gen Physiol* **133**: 245–249
- Chemin J, Monteil A, Briquaire C, Richard S, Perez-Reyes E, Nargeot J, Lory P (2000) Overexpression of T-type calcium channels in HEK-293 cells increases intracellular calcium without affecting cellular proliferation. *FEBS Lett* **478**: 166–172
- del Camino D, Murphy S, Heiry M, Barrett LB, Earley TJ, Cook CA, Petrus MJ, Zhao M, D'Amours M, Deering N, Brenner GJ, Costigan M, Hayward NJ, Chong JA, Fanger CM, Woolf CJ, Patapoutian A, Moran MM (2010) TRPA1 contributes to cold hypersensitivity. *J Neurosci* **30**: 15165–15174
- Dhaka A, Murray AN, Mathur J, Earley TJ, Petrus MJ, Patapoutian A (2007) TRPM8 is required for cold sensation in mice. *Neuron* **54**: 371–378
- Dittert I, Benedikt J, Vyklicky L, Zimmermann K, Reeh PW, Vlachova V (2006) Improved superfusion technique for rapid cooling or heating of cultured cells under patch-clamp conditions. *J Neurosci Methods* **151**: 178–185
- Fleming LE, Baden DG, Bean JA, Weisman R, Blythe DG (1998) Seafood toxin diseases: issues in epidemiology and community outreach. In *Harmful Algae*, Reguera B, Blanco J, Fernandez ML, Wyatt T (eds), pp 245–248. Zunta de Galicia and Intergovernmental Oceanographic Commission of UNESCO
- Gentry C, Stoakley N, Andersson DA, Bevan S (2010) The roles of iPLA2, TRPM8 and TRPA1 in chemically induced cold hypersensitivity. *Mol Pain* **6**: 4
- Griffin JD, Boulant JA (1995) Temperature effects on membrane potential and input resistance in rat hypothalamic neurones. *J Physiol* **488**(Pt 2): 407–418
- Hess A, Axmann R, Rech J, Finzel S, Heindl C, Kreitz S, Sergeeva M, Saake M, Garcia M, Kollias G, Straub RH, Sporns O, Doerfler A, Brune K, Schett G (2011) Blockade of TNF-alpha rapidly inhibits pain responses in the central nervous system. *Proc Natl Acad Sci USA* **108**: 3731–3736
- Hoffman PA, Granade HR, McMillan JP (1983) The mouse ciguatoxin bioassay: a dose-response curve and symptomatology analysis. *Toxicol* **21**: 363–369
- Jordt SE, Bautista DM, Chuang HH, McKemy DD, Zygmunt PM, Hogestatt ED, Meng ID, Julius D (2004) Mustard oils and cannabinoids excite sensory nerve fibres through the TRP channel ANKTM1. *Nature* **427**: 260–265
- Karashima Y, Talavera K, Everaerts W, Janssens A, Kwan KY, Vennekens R, Nilius B, Voets T (2009) TRPA1 acts as a cold sensor in vitro and in vivo. *Proc Natl Acad Sci USA* **106**: 1273–1278
- Kim T, Choi J, Kim S, Kwon O, Nah SY, Han YS, Rhim H (2004) The biochemical activation of T-type Ca²⁺ channels in HEK293 cells stably expressing alpha1G and Kir2.1 subunits. *Biochem Biophys Res Commun* **324**: 401–408
- Knabl J, Witschi R, Hosl K, Reinold H, Zeilhofer UB, Ahmadi S, Brockhaus J, Sergejeva M, Hess A, Brune K, Fritschy JM, Rudolph U, Mohler H, Zeilhofer HU (2008) Reversal of pathological pain through specific spinal GABAA receptor subtypes. *Nature* **451**: 330–334
- Knowlton WM, Bifolck-Fisher A, Bautista DM, McKemy DD (2010) TRPM8, but not TRPA1, is required for neural and behavioral responses to acute noxious cold temperatures and cold-mimetics in vivo. *Pain* **150**: 340–350
- Kwan KY, Glazer JM, Corey DP, Rice FL, Stucky CL (2009) TRPA1 modulates mechanotransduction in cutaneous sensory neurons. *J Neurosci* **29**: 4808–4819

- Lewis RJ (2001) The changing face of ciguatera. *Toxicon* **39**: 97–106
- Lewis RJ, Holmes MJ (1993) Origin and transfer of toxins involved in ciguatera. *Comp Biochem Physiol C* **106**: 615–628
- Lewis RJ, Sellin M (1993) Recovery of ciguatoxin from fish flesh. *Toxicon* **31**: 1333–1336
- Lewis RJ, Sellin M, Poli MA, Norton RS, MacLeod JK, Sheil MM (1991) Purification and characterization of ciguatoxins from moray eel (*Lycodontis javanicus*, Muraenidae). *Toxicon* **29**: 1115–1127
- Lorenz J, Cross DJ, Minoshima S, Morrow TJ, Paulson PE, Casey KL (2002) A unique representation of heat allodynia in the human brain. *Neuron* **35**: 383–393
- Maingret F, Lauritzen I, Patel AJ, Heurteaux C, Reyes R, Lesage F, Lazdunski M, Honore E (2000) TREK-1 is a heat-activated background K(+) channel. *EMBO J* **19**: 2483–2491
- McKemy DD, Neuhauss WM, Julius D (2002) Identification of a cold receptor reveals a general role for TRP channels in thermosensation. *Nature* **416**: 52–58
- Minta A, Kao JP, Tsien RY (1989) Fluorescent indicators for cytosolic calcium based on rhodamine and fluorescein chromophores. *J Biol Chem* **264**: 8171–8178
- Munns C, AlQatari M, Koltzenburg M (2007) Many cold sensitive peripheral neurons of the mouse do not express TRPM8 or TRPA1. *Cell Calcium* **41**: 331–342
- Nagata K, Duggan A, Kumar G, Garcia-Anoveros J (2005) Nociceptor and hair cell transducer properties of TRPA1, a channel for pain and hearing. *J Neurosci* **25**: 4052–4061
- Nassini R, Gees M, Harrison S, De Siena G, Materazzi S, Moretto N, Failli P, Preti D, Marchetti N, Cavazzini A, Mancini F, Pedretti P, Nilius B, Patacchini R, Geppetti P (2011) Oxaliplatin elicits mechanical and cold allodynia in rodents via TRPA1 receptor stimulation. *Pain* **152**: 1621–1631
- Neely GG, Hess A, Costigan M, Keene AC, Goulas S, Langeslag M, Griffin RS, Belfer I, Dai F, Smith SB, Diatchenko L, Gupta V, Xia CP, Amann S, Kreitz S, Heindl-Erdmann C, Wolz S, Ly CV, Arora S, Sarangi R *et al* (2010) A genome-wide *Drosophila* screen for heat nociception identifies alpha2delta3 as an evolutionarily conserved pain gene. *Cell* **143**: 628–638
- Parra A, Madrid R, Echevarria D, del Olmo S, Morenilla-Palao C, Acosta MC, Gallar J, Dhaka A, Viana F, Belmonte C (2010) Ocular surface wetness is regulated by TRPM8-dependent cold thermoreceptors of the cornea. *Nat Med* **16**: 1396–1399
- Peier AM, Moqrich A, Hergarden AC, Reeve AJ, Andersson DA, Story GM, Earley TJ, Dragoni I, McIntyre P, Bevan S, Patapoutian A (2002) A TRP channel that senses cold stimuli and menthol. *Cell* **108**: 705–715
- Reid G (2005) ThermoTRP channels and cold sensing: what are they really up to? *Pflugers Arch* **451**: 250–263
- Reid G, Flonta M (2001) Cold transduction by inhibition of a background potassium conductance in rat primary sensory neurones. *Neurosci Lett* **297**: 171–174
- Seifert F, Maihöfner C (2007) Representation of cold allodynia in the human brain - a functional MRI study. *Neuroimage* **35**: 1168–1180
- Story GM, Peier AM, Reeve AJ, Eid SR, Mosbacher J, Hricik TR, Earley TJ, Hergarden AC, Andersson DA, Hwang SW, McIntyre P, Jegla T, Bevan S, Patapoutian A (2003) ANKTM1, a TRP-like channel expressed in nociceptive neurons, is activated by cold temperatures. *Cell* **112**: 819–829
- Strachan LC, Lewis RJ, Nicholson GM (1999) Differential actions of pacific ciguatoxin-1 on sodium channel subtypes in mammalian sensory neurons. *J Pharmacol Exp Ther* **288**: 379–388
- Viana F, de la Pena E, Belmonte C (2002) Specificity of cold thermotransduction is determined by differential ionic channel expression. *Nat Neurosci* **5**: 254–260
- Voets T, Droogmans G, Wissenbach U, Janssens A, Flockerzi V, Nilius B (2004) The principle of temperature-dependent gating in cold- and heat-sensitive TRP channels. *Nature* **430**: 748–754
- Wilson SR, Gerhold KA, Bifolck-Fisher A, Liu Q, Patel KN, Dong X, Bautista DM (2011) TRPA1 is required for histamine-independent, Mas-related G protein-coupled receptor-mediated itch. *Nat Neurosci* **14**: 595–602
- Yamaoka K, Inoue M, Miyazaki K, Hirama M, Kondo C, Kinoshita E, Miyoshi H, Seyama I (2009) Synthetic ciguatoxins selectively activate Nav1.8-derived chimeric sodium channels expressed in HEK293 cells. *J Biol Chem* **284**: 7597–7605
- Zimmermann K, Hein A, Hager U, Kaczmarek JS, Turnquist BP, Clapham DE, Reeh PW (2009) Phenotyping sensory nerve endings in vitro in the mouse. *Nat Protoc* **4**: 174–196
- Zimmermann K, Leffler A, Babes A, Cendan CM, Carr RW, Kobayashi J, Nau C, Wood JN, Reeh PW (2007) Sensory neuron sodium channel Nav1.8 is essential for pain at low temperatures. *Nature* **447**: 855–858
- Zimmermann K, Lennerz JK, Hein A, Link AS, Kaczmarek JS, Delling M, Uysal S, Pfeifer JD, Riccio A, Clapham DE (2011) Transient receptor potential cation channel, subfamily C, member 5 (TRPC5) is a cold-transducer in the peripheral nervous system. *Proc Natl Acad Sci USA* **108**: 18114–18119
- Zurberg S, Yurgionas B, Jira JA, Caspani O, Heppenstall PA (2007) Direct activation of the ion channel TRPA1 by Ca²⁺. *Nat Neurosci* **10**: 277–279